Niğde Ömer Halisdemir Üniversitesi Mühendislik Bilimleri Dergisi
Niğde Ömer Halisdemir University Journal of Engineering Sciences

Araştırma makalesi / Research article

www.dergipark.org.tr/tr/pub/ngumuh / www.dergipark.org.tr/en/pub/ngumuh

A novel Dual-Wideband bandstop filter based on three-port nested dual-mode resonators with tunable notch band and distinct filtering characteristics

Üç portlu Dual-Mod rezonatörler kullanılarak tasarlanan, ayarlanabilir çentik bantlı ve farklı filtreleme karakteristiğine sahip yeni bir çift geniş bantlı bant durduran filtre

Elif Güntürkün Şahin[1,*]

[1] *Niğde Ömer Halisdemir Üniversitesi, Elektrik Elektronik Mühendisliği Bölümü, 51240, Niğde Türkiye*

Abstract

In this paper, a novel three-port wideband bandstop filter is designed using two nested dual-mode resonators. The resonators share a common side and are fed by the direct-coupling method, thereby exciting the degenerate modes to obtain a wideband frequency response. Two distinct filtering characteristics are obtained by employing perturbation and reference elements along the edges of the filter, while the bandwidth and notched-band frequency are controlled by varying the values of these elements. These elements are realized by combining lumped and distributed capacitances. To reveal the operating mechanism of the proposed filter topology, the even–odd-mode equivalent circuit of a single loop resonator is obtained and analyzed. The resonator with capacitive loading elements is investigated under weak coupling conditions through simulation. The filter exhibits two wide stopbands in the S_{11} response with center frequencies of 0.96 GHz and 3.17 GHz and fractional bandwidths of 104% and 60%, respectively, while a passband with a center frequency of 1.84 GHz and a fractional bandwidth of 76% is achieved between the two stopbands. In the S_{33} response, a wideband bandstop response is achieved, and a tunable notched band with a center frequency of 3.011 GHz and a bandwidth of 20 MHz is realized in both filtering characteristics. The frequency response of the filter is obtained using simulation, showing that the proposed filter has a compact size of 33.4 × 26.5 mm² and exhibits high performance.

Anahtar kelimeler: Microwave filter, Bandstop, Tunable notch band, 3-port

Öz

Bu çalışmada yeni bir iç içe geçmiş dual-mod rezonatörler kullanılarak, üç-portlu geniş çift band bant durduran filtre tasarlanmıştır. Rezonatörlerin bir kenarları ortak olup, direkt kuplaj metoduyla beslenmiş, bu şekilde dejenere modlar uyarılarak geniş band frekans cevabı elde edilmiştir. Filtre kenarları üzerinde pertürbasyon ve referans elemanları kullanılarak iki farklı filtreleme karakteristiği elde edilmiş ve bu elemanların değerlerinin değişimi ile band genişliği ve çentik bandın frekans kontrolü sağlanmıştır. Bu elemanlar, toplu ve dağınık tipte kapasitelerin birlikte kullanılmasından oluşmuştur. Önerilen filtre topolojisinin çalışma mekanizmasını ortaya koymak amacıyla, tek bir halka rezonatörün even–odd mod eşdeğer devresi elde edilmiş ve analiz edilmiştir. Kapasitif yükleme elemanlarına sahip rezonatör, zayıf kuplaj koşulları altında benzetim yoluyla incelenmiştir. Filtre, S_{11} cevabında sırasıyla 0.96 GHz ve 3.17 GHz merkez frekanslarında ve %104 ve %60 kısmi band genişliklerine sahip iki geniş band tutma bandına sahip bir cevap verirken, bandlar arası merkez frekansı 1.84 GHz, %76 kısmi band genişliğinde bir geçme bandına sahiptir. S_{33} cevabında genişband band durduran ve her iki karakteristikte 3.011 GHz frekansında ve 20 MHz band genişliğinde ayarlanabilir çentik band oluşturulmuştur. Filtrenin frekans cevabı benzetim programı yardımıyla elde edilmiş olup, 33.4 x 26.5 mm2 boyutunda, oldukça kompakt yapıda ve yüksek performanslı bir filtre olduğu görülmektedir.

Keywords: Mikrodalga filtre, Band tutan, Ayarlanabilir çentik bant, 3-port

1 Introduction

With recent developments in modern communication systems, there is an increasing demand for tunable and reconfigurable multifunctional microwave components, such as oscillators, diplexers, filters, filtennas, and antennas, featuring compact size and high performance. Tunable bandstop filters with a notch band play a critical role among these components, as they suppress unwanted signals and interference while allowing only a narrow passband within the stopband.

In the literature, numerous filter designs with reconfigurable and tunable characteristics have been reported in various structures, in parallel with recent advances in modern technology, and these studies can be classified into two categories depending on the use of active or passive components. In [1], a wideband dual-band bandstop filter (DBSF) based on coupled lines and open-ended stubs is presented. It is demonstrated that the stopband rejection, bandwidth (BW), and center frequency ratio can be flexibly controlled. Similarly, in [2], an ultra-wideband (UWB) filter realized using coupled lines and open-ended

* Sorumlu yazar / Corresponding author, e-posta / e-mail: elifgunturkun35@hotmail.com (E Güntürkün Şahin)
Geliş / Received: 21.04.2026 Kabul / Accepted: 02.07.2026 Yayımlanma / Published: 03.07.2026
doi: 10.28948/ngumuh.1935370

stubs is presented. Although a very wide frequency range is achieved, the filter exhibits relatively poor performance in terms of out-of-band passband return loss levels. Wideband bandstop filter (WBSF) structures utilizing dual-mode resonators (DMRs) can be found in [3] and [4]. In [3], the degenerate modes of a single DMR are excited by employing direct feeding, and a single-band bandstop response is obtained with the use of loading elements. In [4], nested DMRs are employed to realize WBSF that provide a single-band to dual-band response.

In addition to these WBSF studies, electronically tunable and adjustable filter designs have attracted significant attention and have been widely investigated by researchers for both bandstop and bandpass filter applications. One of these studies is the switchable filter design presented in [5], which is realized using coupled transmission lines. In this work, by employing PIN diodes, the bandstop filter response can be configured as either wideband or dual-band. Similarly, in [6], a reconfigurable filter is proposed using RF-MEMS switching elements, which enables operation from bandpass to bandstop, as well as from single-band to dual-band responses. In this design, variable fractional bandwidth (FBW) and reconfigurable selectivity are achieved by employing circulators and multimode resonators. Moreover, two different filter designs based on stepped-impedance resonators are reported in [7] and [8], corresponding to a UWB bandstop and a dual-band bandpass filter, respectively. Although BW tuning is achieved using varactor diodes, the proposed structures suffer from relatively large physical dimensions.

In addition to all the filter studies discussed above, tunable notch-band filters are widely preferred, particularly in 5G/sub-6 GHz, interference suppression, and cognitive radio applications. Furthermore, tunable notch-band filters have attracted considerable attention due to their ability to effectively suppress unwanted signals within specific frequency bands. In [9], a varactor-loaded DBSF with a tunable notch band is realized using coupled lines. Similarly, in [10], a bandpass filter with an electronically tunable notch band is presented based on stepped-impedance resonators (SIRs). In addition, a filtenna design with a reconfigurable notch band is achieved using an RF switch matrix [11]. However, these studies still face significant challenges in achieving compact size and high selectivity. In [12], an electronically reconfigurable and tunable DBSF employing nested DMRs is presented. Although the reported design allows the adjustment of the notched-band frequency and bandwidth, it provides only a single filtering response, and a second filtering characteristic cannot be achieved.

In this paper, a three-port filter structure is proposed, which provides two distinct filtering responses, along with tunable notch-band characteristics and adjustable bandwidth. For this purpose, similar to [3], a dual-wideband bandstop filter is realized based on nested DMRs with a direct coupling configuration, where perturbation and reference elements are employed. Unlike previous studies in the literature, a third port is introduced along the symmetry axis, enabling two distinct filtering characteristics.

The proposed filter responses exhibit a tunable notch band with adjustable resonance frequency and bandwidth. In this structure, the filter response can be effectively controlled by adjusting the values of the perturbation and reference elements, realized by using a hybrid configuration of lumped and distributed capacitive elements.

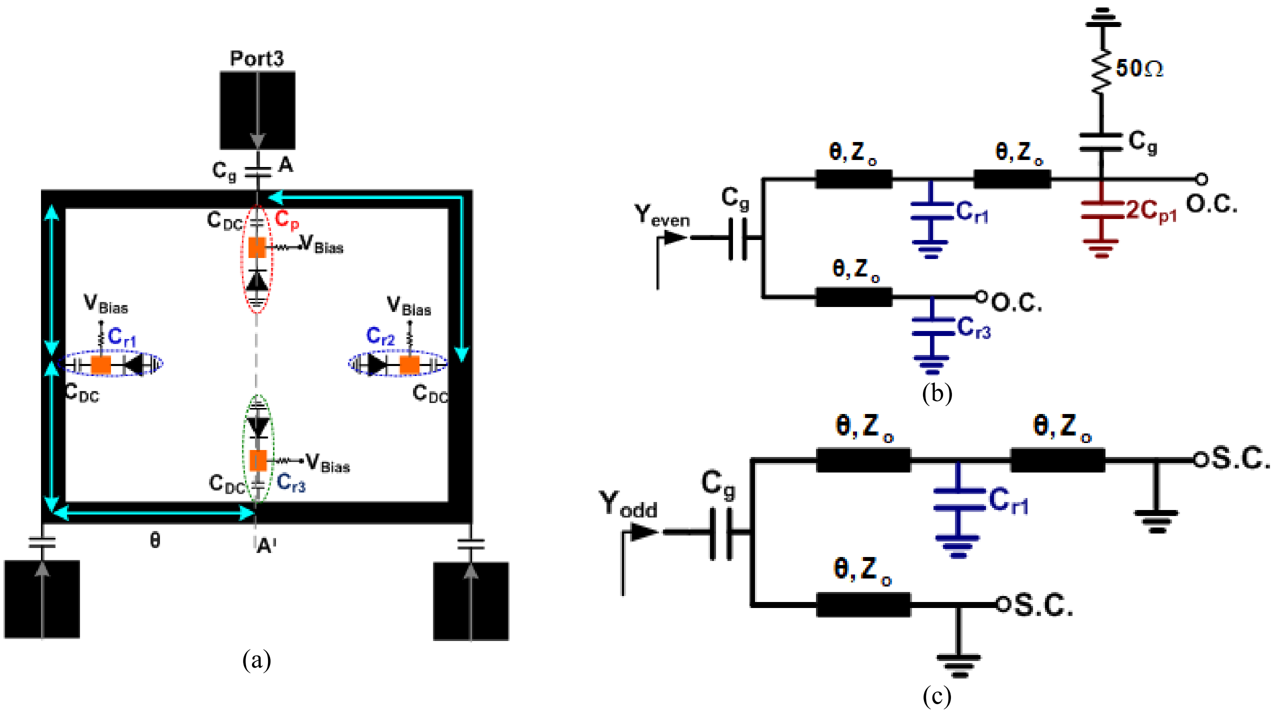

Figure 1. (a) Proposed three-port DMR with capacitances under weak coupling (b) even mode equivalent circuit model (c) odd mode equivalent circuit model

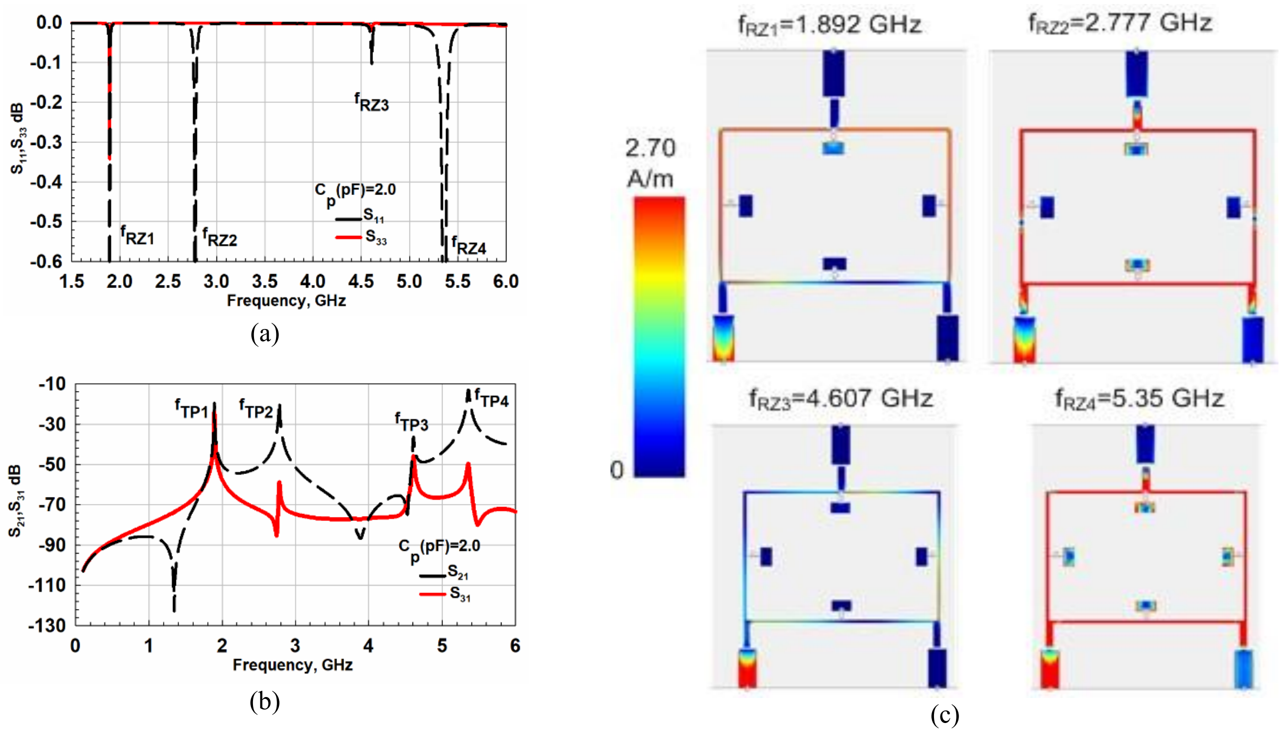

Figure 2. Simulated weak-coupling responses for C_p=2.0 pF (a) S_{11} and S_{33}, (b) S_{21} and S_{31} responses and (c) surface current distributions at f_{RZ1}=1.892 GHz, f_{RZ2}=2.777 GHz, f_{RZ3}=4.607 GHz and f_{RZ4}=5.35 GHz.

2 Tunable notched band filter

2.1 Circuit design

Figure 1(a) illustrates a three-port DMR with lumped capacitive elements, referred to as the perturbation element (C_p) and three reference elements (C_{r1}, C_{r2}, and C_{r3}). The proposed filter differs from existing designs in the literature, such as [3], in that it includes an additional port along the symmetry axis and has a third reference element. The proposed resonator is excited under weak coupling to reveal the degenerate modes of the DMR.

To reveal the characteristics of the design, even-odd mode equivalent circuit models are given in Figure 1(b) and (c). As is well known from [13], a DMR supports DMs, and the filter characteristic (elliptic, linear, etc.) can be adjusted by controlling the coupling type (electric, magnetic, or balanced). The following equations are used to determine the input admittances of the even and odd mode (Y_{even} and Y_{odd}) equivalent circuits depicted in Figures 1(b) and 1(c). Unlike the structure reported in [12], the proposed topology introduces a third port on the symmetry plane. Since this port introduces an additional loading effect on the resonator, it is represented by a 50-Ω termination in the equivalent circuit model. Y_{even} and Y_{odd} are given in following equations to calculate the resonance conditions, respectively.

$$Y_{even} = \left[\frac{1}{j\omega C_g} + \frac{1}{Y_{be} + Y_{te}}\right]^{-1} \quad (1)$$

where Y_{te} Y_{be}, Y_{L1} are

$$Y_{te} = Y_o \frac{\left[j\omega C_{r1} + Y_o \frac{Y_L + jY_o \tan(\theta)}{Y_o + jY_L \tan(\theta)}\right] + jY_o \tan(\theta)}{Y_o + j\tan(\theta)\left[j\omega C_{r1} + Y_o \frac{Y_L + jY_o \tan(\theta)}{Y_o + jY_L \tan(\theta)}\right]} \quad (2)$$

$$Y_{be} = Y_o \frac{j\omega C_{r3} + jY_o \tan(\theta)}{Y_o + j(j\omega C_{r3})\tan(\theta)} \quad (3)$$

$$Y_L = j\omega(2Cp) + \frac{1}{50 + \frac{1}{j\omega Cg}} \quad (4)$$

Additionally, Yodd admintance can be expressed as,

$$Y_{odd} = \left[\frac{1}{j\omega C_g} + \frac{1}{Y_{bo} + Y_{to}}\right]^{-1} \quad (5)$$

$$Y_{to} = Y_o \frac{j\omega C_{r1} - jY_o \cot(\theta) + jY_o \tan(\theta)}{Y_o + j\left(j\omega C_{r1} - jY_o \cot(\theta)\right)\tan\theta} \quad (6)$$

$$Y_{bo} = -jY_o \cot(\theta) \quad (7)$$

Here, Y_o and θ denote the characteristic admittance and electrical length of the transmission-line sections, respectively. C_p represents the perturbation capacitance, whereas C_{r1}, C_{r2} and C_{r3} denote the reference capacitance elements. For the even odd mode analysis, C_{r1} and C_{r2} are chosen to have identical values and are placed symmetrically with respect to the symmetry plane.

Firstly, to reveal the filtering characteristic, the variation of C_p=2.0 pF is investigated in terms of its effect on the frequency response of the DMR, while the reference elements are fixed at 0 pF. Figure 2(a) shows this effect on S-parameters. As can be seen from the figure, this design exhibits four reflection zeros (RZs), denoted as f_{RZ1}=1.892 GHz, f_{RZ2}=2.777 GHz, f_{RZ3}=4.607 GHz and f_{RZ4}=5.35 GHz. These four RZs appear in the S_{11} response, whereas in the S_{33} response, only f_{RZ1} and f_{RZ3} are observed and they are the same as those in S11.

Figure 2(a) and (b) shows the effect the mode frequencies of the single resonator under weak coupling. Therefore, the reflection zeros observed in Figure 1(a) indicate the resonant modes of the resonator. In the proposed three-port topology, the third port is not a symmetry boundary but a physically connected port terminated with the standard port impedance. Hence, its 50 Ω loading effect is included in the even odd mode equivalent circuit. This approach allows the mode behavior obtained under weak coupling to be related to the attenuation poles and notch behavior observed in the directly coupled three-port bandstop filter.

Also, Figure 1(c) shows the current distributions of the RZs, where the current magnitude is normalized to a maximum value of 2.70 A/m. Here, at the frequencies of f_{RZ1} and f_{RZ3}, the S_{11} and S_{33} responses indicate the impedance matching which leads to maximum transmission between the ports and the resonator. However, at the remaining frequencies, the lack of RZs in the S_{33} response implies that the corresponding modes are more strongly excited from Port1, whereas the coupling from Port3 is relatively weaker. Furthermore, transmission poles (TPs) observed in the S_{21} and S_{31} responses at the corresponding frequencies indicate that transmission between the ports occurs at these frequencies. Furthermore, [4] demonstrated that the TZs generated by a DMR under weak-coupling conditions are transformed into APs through a direct-coupling mechanism. A comparable behavior is observed in the proposed filter structure, where the reflection zeros obtained from the weakly coupled resonator configuration are converted into transmission poles due to the introduced direct-coupling path.

2.2 Resonator analysis

To examine the effect of the perturbation and reference elements on the resonant characteristics, each parameter is varied individually with the remaining elements fixed at 0 pF. Figure 3 (a), (b) and (c) show the S_{21} frequency responses corresponding to the variations of C_{p1}, C_{r1}=C_{r2} and C_{r3}, respectively. It can be seen from the figures that the DMR exhibits four TPs denoted as f_{TP1}, f_{TP2}, f_{TP3} and f_{TP4}. According to the simulation results, these frequencies are equal to the previously identified RZs.

From Figure 3(a), it is observed that as the value of C_{p1} increases, f_{TP2} and f_{TP4} remain stable in frequency, whereas the remaining TP shift toward lower frequencies. And also, to maintain the symmetry of the structure C_{r1} and C_{r2} are kept equal, and it is observed that increasing these capacitances causes all TP, except f_{TP2}, to shift toward lower frequencies as show in Figure 3(b).

In Figure 3(c), the effect of varying C_{r3} is examined, and the movement of the TPs along the frequency axis is found to be similar to that observed for C_P. Additionally, with increasing capacitance, the transmission zeros (TZs) shift from the real axis toward the imaginary axis.

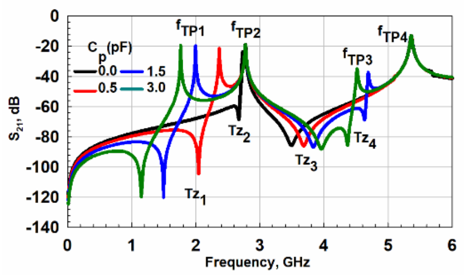

(a)

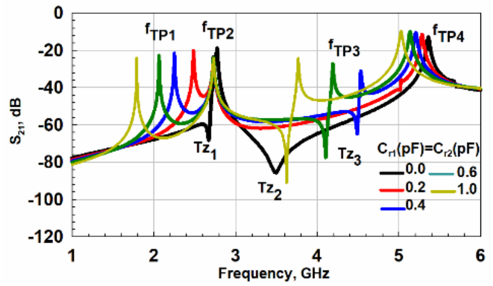

(b)

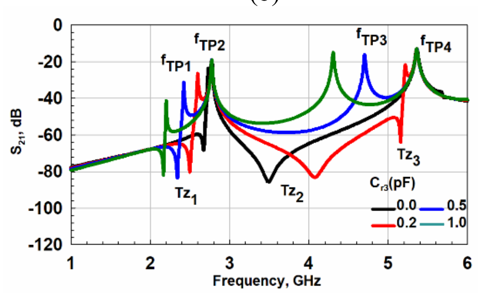

(c)

Figure 3. Simulated S-parameter responses for different values of (a) C_p (b) C_{r1}=C_{r2} , and (c) C_{r3}.

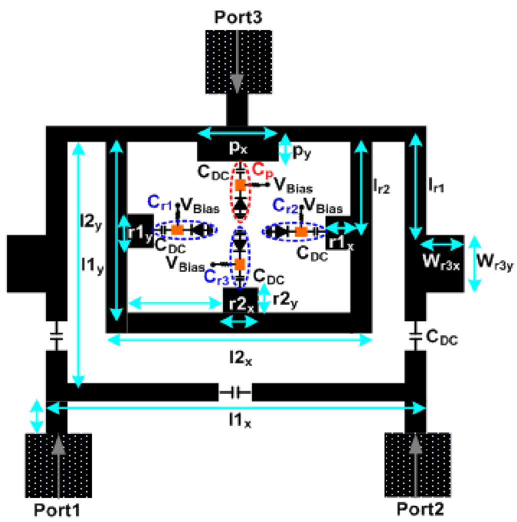

Figure 4. Layouts of the proposed three-port nested DMR

2.3 Notched band bandstop filter design

A novel three-port bandstop filter design layout is presented in Figure 4. This structure consists of two nested DMRs sharing a common edge where a perturbation elements denoted as C_P is located. The inner resonator includes three reference elements denoted as C_{r1}, C_{r2} and C_{r3} while the outer resonator has two identical conductor patches with dimensions W_{r3x} and W_{r3y}. In this study, the parametric behavior of the proposed structure was investigated through simulation results. The perturbation and reference elements were implemented using varactor diodes, and their effects were examined by varying the corresponding capacitance values.

To ensure the proper excitation of the degenerate modes of DMRs, capacitive elements are employed in a hybrid configuration of lumped and distributed capacitive elements. In this design, C_{p1}=C_{r1}=C_{r2}=1.5 pF are employed on capacitive conductor patches. In this way, the proposed design combines distributed capacitive elements with lumped circuit components. Here, the direct coupling method is employed to provide the required coupling between the DMRs and to obtain wideband bandstop frequency response with tunable notched band.

The proposed design exhibits two distinct filtering characteristics in its S_{11} and S_{33} frequency responses. Here, a dual-wideband bandstop filter comprising two stopbands, referred to as Stopband1 and Stopband2, is realized between Port1 and Port2, with a passband located between them, whereas a wideband bandstop response is observed between Port1 and Port3. Each response features a tunable notched band operating at the same frequency.

Figure 5(a) presents the S-parameter and phase responses corresponding to each parameter variation (C_p, C_{r1}=C_{r2}, and W_{r3}x-W_{r3y}). First, considering the S_{11}/S_{21} magnitude responses shown in Figure 5(a), the overall bandwidth remains nearly unchanged, whereas the lower cut-off frequency of the first stopband shifts toward lower frequencies as C_p increases. In contrast, the S_{33}/S_{31} responses exhibit a distinct dependence on C_p. The notched-band response observed around 3 GHz is suppressed, while another notch response appears around 1.5 GHz. As a result, the S_{33} response exhibits a high-pass filtering characteristic. This effect is also reflected in the corresponding phase responses. While the phase transition associated with the notch around 3 GHz is reduced, another phase transition is observed near 1.5 GHz. These observations indicate that the capacitance C_p modifies the mode interaction within the resonator and consequently provides an adjustable notch response over different frequency regions.

As in Figure 5(a), Figure 5(b) presents the S-parameter magnitude (dB) and phase responses for different values of C_{r1}=C_{r2}. As C_{r1}=C_{r2} increases, the notched band frequencies and filtering bands shift toward lower frequencies. A similar effect is observed in the corresponding phase responses. These results indicate that C_{r1}=C_{r2} mainly provides frequency tuning of the notch and filtering responses.

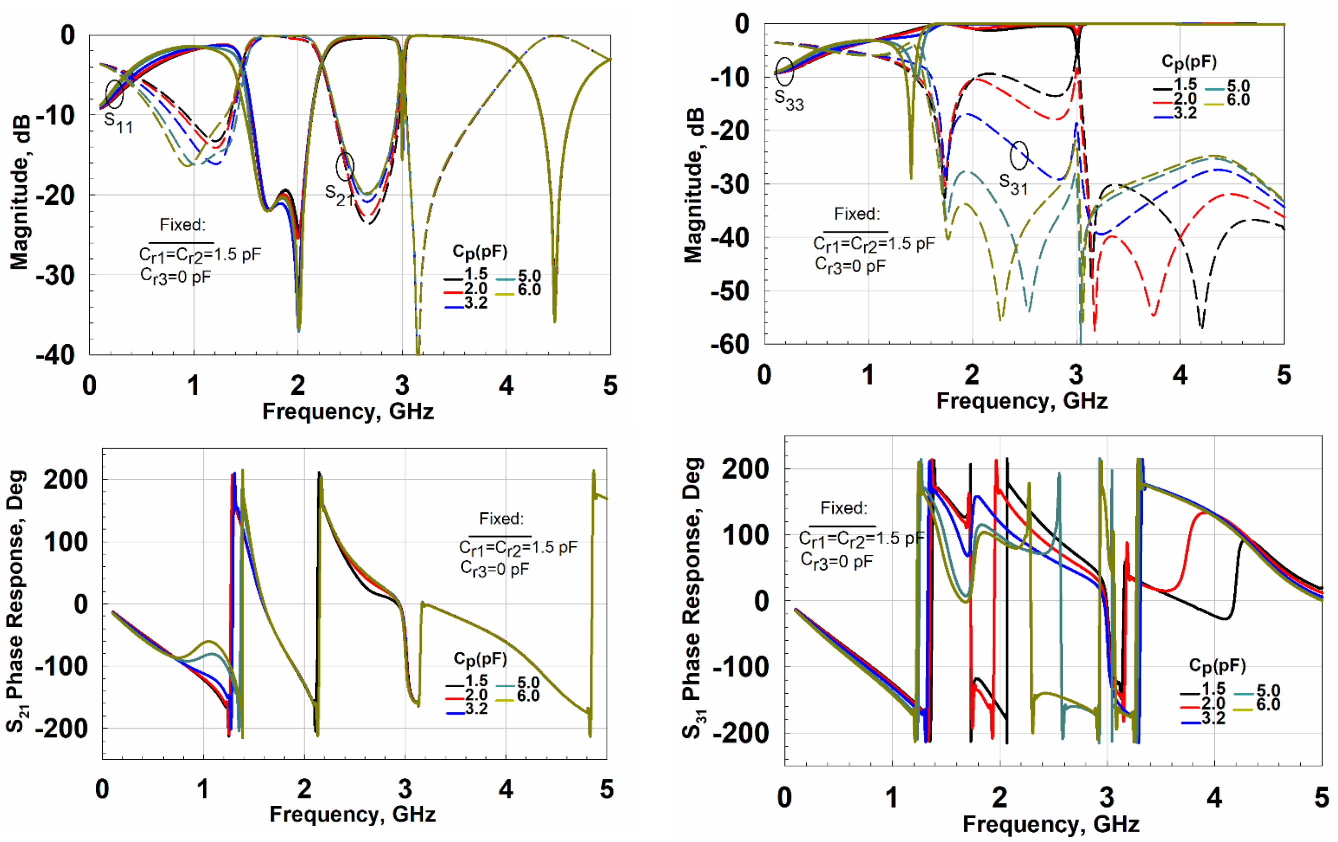

(a)

Figure 5. Simulated S-parameter magnitude and phase responses of the proposed three-port filter (a) Cp, (b) Cr1=Cr2 and (c) Wr3y for a fixed Wr3x=4.0 mm

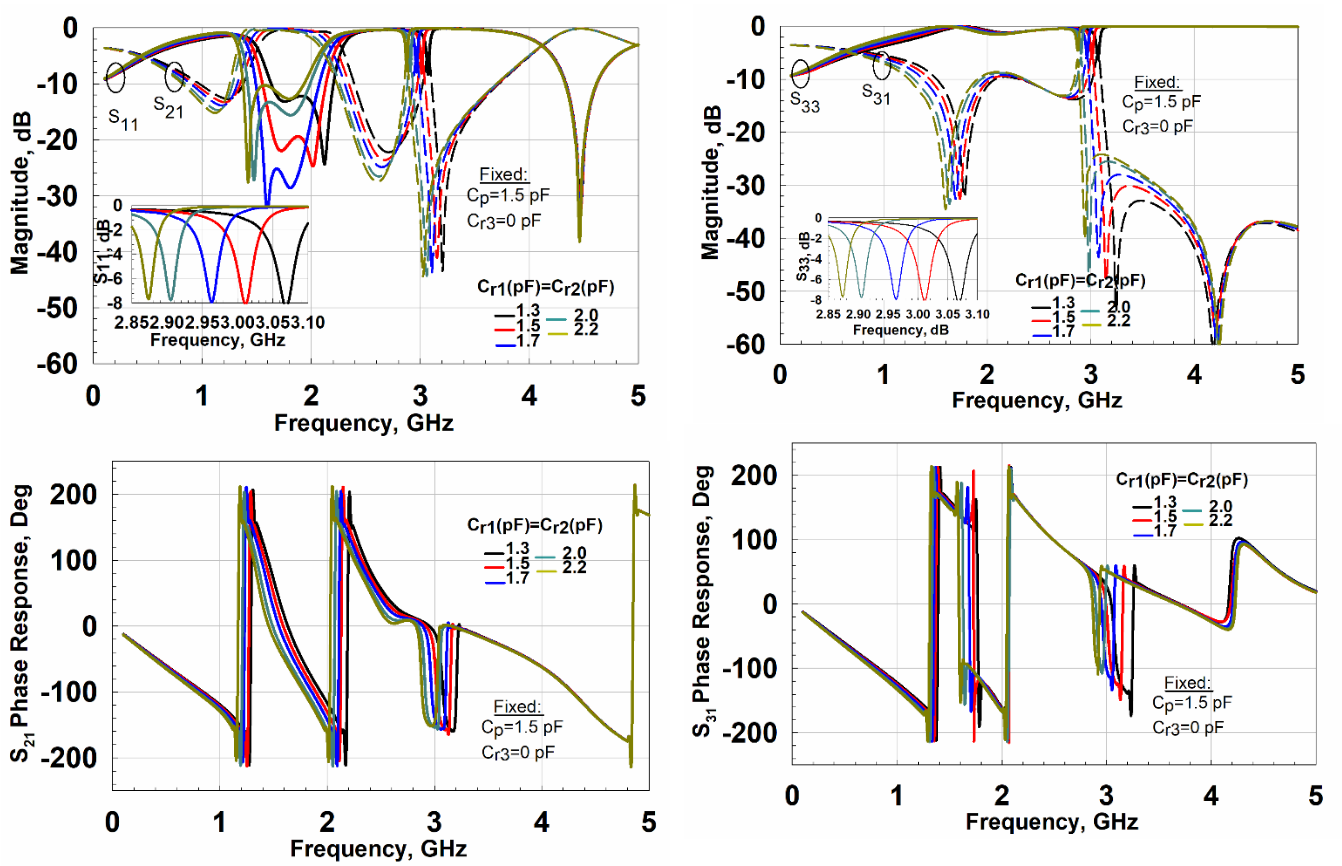

(b)

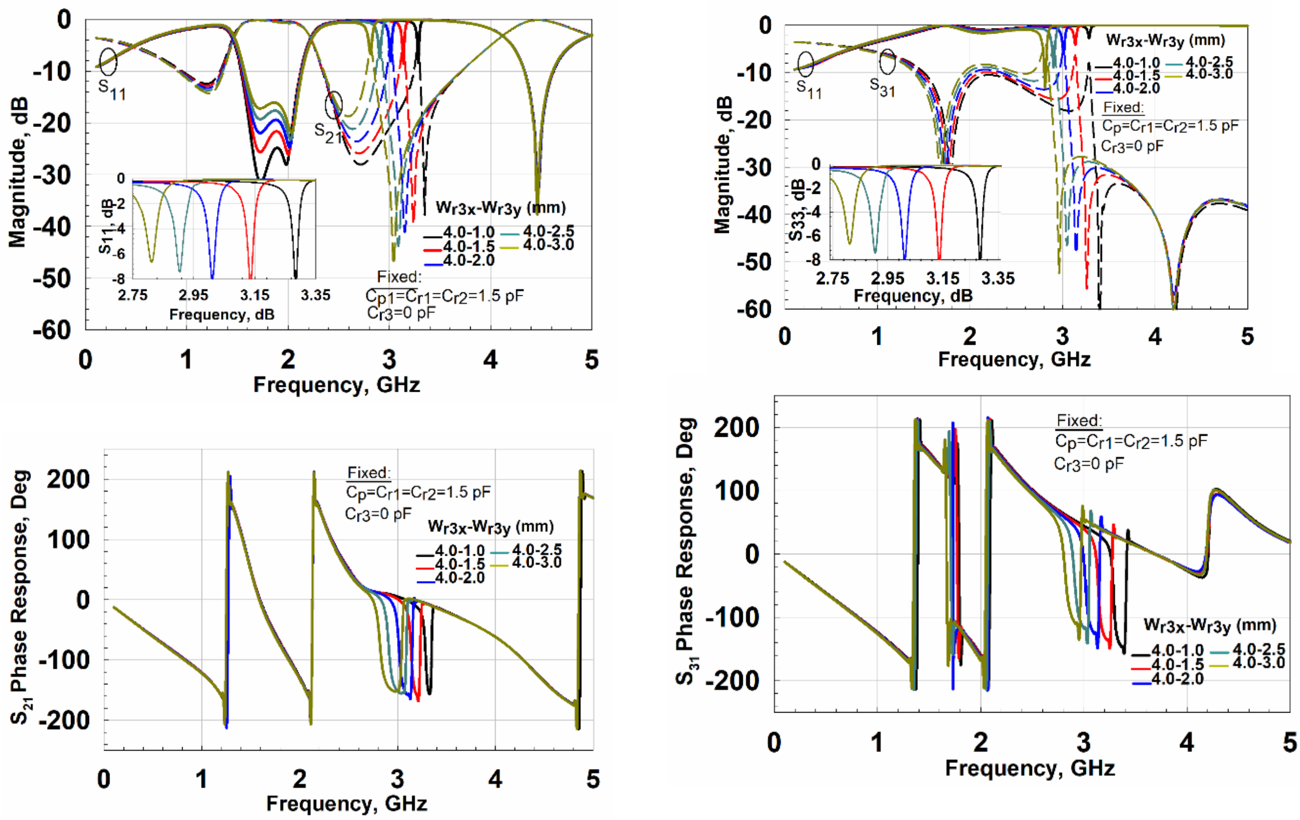

(c)

Figure 5 (continued). Simulated S-parameter magnitude and phase responses of the proposed three-port filter (a) Cp, (b) Cr1=Cr2 and (c) Wr3y for a fixed Wr3x=4.0 mm

Similar to the results presented in Figure 5(a) and (b). shows the S-parameter magnitude (dB) and phase responses for different values of W_{r3y}, while W_{r3x} is kept constant at 4.0 mm. As W_{r3y} increases, the notched-band frequencies and filtering bands shift toward lower frequencies without significantly affecting the overall filtering response. The same behavior is observed in the corresponding phase.

3 Results and discussions

The proposed three-port wideband bandstop filter has two distinct filtering characteristic. In S_{11} and S_{21}, responses, the filter provides a dual-wideband bandstop response with a wide passband between the stopbands and a tunable notched band within one of the stopbands. On the other hand, the S_{33} response exhibits a wideband bandstop characteristic with a tunable notched band, similar to that observed in the S_{11} response. By utilizing the perturbation and reference elements, the operating frequency of the notched band can be tuned either independently or simultaneously with the center frequencies of the passband and stopbands, while the whole bandwidth of the filter remains constant.

A full-wave electromagnetic simulator [14] was used to analyze the proposed filter design on a Rogers RT/Duroid 4003 Cu substrate with a thickness of 0.813 mm and a relative permittivity of ε_r=3.55. The dimensions of the filter are (in mm) $l1_x$=19.4, $l1_y$=13.5, $l2_x$=17, $l2_y$=12.4, l_{r1}=5.3, l_{r3}=3.4, l_b=2.5, p_x=6.2, p_y=1.5, $r1_x$=3.0, $r1_y$=4.4, $r2_x$=4.0, $r2_y$=2.0, W_{r3x}=7.0, W_{r3y}=5.6. Table 1 presents the simulated results of the proposed filter. The designed filter demonstrates good performance in terms of both compact size and filtering characteristic. Compared with previously reported tunable bandstop filters, the proposed design not only provides frequency tuning but also offers two distinct filtering characteristics while maintaining a tunable notched-band response. A comparison with previously reported bandstop filters is presented in Table 2. The proposed filter integrates dual-wideband bandstop responses, tunable notch-band operation, and two distinct filtering characteristics within a compact three-port structure, offering greater functional versatility than conventional bandstop filter designs.

4 Conclusions

In this study, a novel three-port wideband bandstop filter with distinct filtering characteristic and a tunable notched band is proposed using nested DMRs. A direct coupling method is employed to achieve the required coupling between the resonators. Additionally, capacitive elements with a hybrid configuration of lumped and distributed capacitances denoted as perturbation and reference elements are utilized to necessary coupling to the resonators and control the resonant modes of the structure. Unlike conventional filters, the proposed design has a third port located the symmetry axis, resulting in two distinct frequency responses in terms of S_{11} and S_{33}. By properly selecting the dimensions of the perturbation and reference elements, the notched band operating frequency in both responses are tuned either independently or simultaneously with the passband and stopbands frequencies. This capability enables the realization of dual responses from a single filter structure, offering enhanced flexibility in frequency control. Therefore, the proposed filter presents a notable advantages for next generation communication systems, requiring reconfigurable and multifunctional filtering characteristics. To validate the design, the filter simulated and the obtained results demonstrate good performances.

Table 1. Summary of the center frequency (f_o), fractional bandwidth (FBW), and insertion loss (RL) for each band of the dual-wideband filter.

	f_o (GHz)	RL (dB)	% FBW
Stopband1	0.96	-1.21	1.04
Stopband2	3.17	-0.08	60
Passband	1.84	-0.11	41
Notched Band	3.011	-4.76	0.66

Tablo 2 Comparison table

Ref. No.	Band Type	Tunable	Reconfigurable	fo (GHz)	BW (MHz)	Size	Notched Band
[9]	Dual BSF	Yes	No	1.2–1.9/ 2.5–3.3	310 ± 30 /720 ± 20	9×27.5 mm² (0.07λg × 0.213λg)	No
[7]	Tunable UWB BSF	Yes	No	6.045	7210	0.23λg×0.32λg	No
[5]	Dual/Wideband BSF	Yes	Yes	0.933-2.414 /1.053-2.351 /4.65	118.1	52.6×56.4 mm² (0.26 λg²)	No
[10]	Triple Band BPF	Yes	No	3.65/4.65/5.4	740/610/ 240	15x30 mm²	Yes
[6]	Dual BSF	Yes	Yes	0.72 / 1.11	67 / 44	56.9 × 24.9 mm²	No
Proposed Work	Dual Wideband BSF	Yes	Yes (Two Distinct Filtering Characteristics)	0.96/3.17	1.04 / 1.54	33.4×26.5 mm² 0.45λg × 0.31λg	Yes

CRediT authorship contribution statement

Elif Güntürkün Şahin: Investigation, Data curation, Formal analysis, Methodology, Validation, Writing – original draft, Writing–review and editing.

Conflict of interest

The authors declare that they have no conflict of interest.

Similarity Rate (iThenticate): 15%

Declaration of generative artificial intelligence (AI) and AI-assisted technologies in the writing process

The author did not use any artificial intelligence tools in the preparation of this work.

References

[1] C. Xu, X. Wang, L. Zhu, W. Sun, K. Li, G. Milinevsky, and G. Lu, "A wideband dual-band bandstop filter with flexible control of stopband rejection, bandwidth and centre frequency ratio," *IET Microwaves, Antennas & Propagation*, 18, pp. 308-316, 2024, doi: 10.1049/mia2.124 51.

[2] O. M. Dardeer, H. A. Elsadek, H. M. Elhennawy, and E. S. Abdallah, "Ultra-wideband bandstop filter with multiple transmission zeros using in-line coupled lines for 4G/5G mobile applications," *International Journal of Electronics and Communications*, 131, p. 153635, 2021, https://doi.org/10.1016/j.aeue.2021.153635

[3] E. Güntürkün Şahin, A. K. Görür, C. Karpuz and A. Gorur, “A novel compact wideband bandstop filter design using a dual-mode square loop resonator”. *Asia-Pacific Microwave Conference*, pp: 1-4, New Delhi, 5-9, 2016. doi:10.1109/APMC.2016.793 1430

[4] E. Güntürkün Şahin, “A reconfigurable and tunable single to dual wideband bandstop filter by using nested dual-mode square loop resonator”. *International Journal of Electronics and Communications*, 68, (154710), 2023. https://doi.org/10.1016/j.aeue.2023.154710.

[5] H. Mei, X. Zuo, M. He and Y. Li, “A compact switchable bandstop filter with dual-band and wideband bandstop functions.” *Journal of Electromagnetic Waves and Applications*, 39, 594-606, 2025. https://doi.org/10.1080/09205071.2025.2465498

[6] N. Kumar and Y. Kumar Singh, “RF-MEMS-Based bandpass-to-bandstop switchable single- and dual-band filters with variable fbw and reconfigurable selectivity.” 65, (10), pp 3824-3837, 2017. doi: 10.1109/ TMTT.2017.2696004.

[7] A. Rajput and B. Mukherjee, “Electronically tunable UWB bandstop filter using varactor diode”. *International Journal of Electronics and Communications*, 164, (154610), 2023. https://doi.org/10.1016/j.aeue.2023.154610.

[8] B. Pal and S. Dwari, “Microstrip dual-band bandpass filter with independently tunable passbands using varactor-tuned stub loaded resonators.” *International Journal of Electronics and Communications*, 73, pp. 105-109, 2017. http://dx.doi.org/10.1016/j.aeue.2017.01.004.

[9] S. Sedighi Maragheh, M. Dousti, M. Dolatshahi and B. Ghalamkari, “A novel dual-band tunable notch filter with controllable center frequencies and bandwidths.” *International Journal of Electronics and Communications*, 88, pp 70-77, 2018. https://doi.org/10.1016/j.aeue.2018.02.018.

[10] D. S. Bade and S. S. Mande, “Ultra-wideband bandpass filter with electronically tunable notch-band. Advances in Electrical Engineering”, *Electronics and Energy*, 10, (100744), 2024. https://doi.org/10.1016/j.prime.2024.100744.

[11] G. M. Elashry, H. A. Mohammed, A. A. Ammar and E. A. Abdallah, “Cloverleaf filtenna with reconfigurable quintuple rejection bands using defected microstrip structure”. *International Journal of Electronics and Communications*, 168, (154708), 2023. https://doi.org/10.1016/j.aeue.2023.154708.

[12] E. Güntürkün Şahin, “An electronically reconfigurable/tunable dual band bandstop filter for cognitive radio applications”, *Global Power, Energy and Communication Conference* (IEEE GPECOM2025), pp. 964-967, Bochum, 11-13 June 2025. doi:10.1109/GPECOM65896.2025.11062013.

[13] A. Gorur, “Description of coupling between degenerate modes of a dual-mode microstrip loop resonator using a novel perturbation arrangement and its dual-mode bandpass filter applications”. *IEEE Trans on Micro Theory and Techn*. 52(2), p. 671-7, 2004. doi:10.1109/TMTT.2003.822033.

[14] Sonnet User’s Manual, Version 14, Sonnet Software, NY, June 2011.s